American Physiological Society | Journal of Neurophysiology

PUBLISHED ARTICLE
ARCHIVES
SUBSCRIPTIONS
SUBMISSIONS
CONTACT US

J Neurophysiol. 2015 Aug; 114(2): 1041–1047.
Published online 2015 May 27.
doi: 10.1152/jn.00391.2015: 10.1152/jn.00391.2015

PMCID: PMC4725105
PMID: 26019314

Experimental muscle pain increases variability of neural drive to muscle and decreases motor unit coherence in tremor frequency band

Utku Ş. Yavuz,[1,2] Francesco Negro,[2] Deborah Falla,[2] and Dario Farina[2]

[1]Department of Orthobionics, Georg August University, Göttingen, Germany; and
[2]Department of Neurorehabilitation Engineering, Bernstein Focus Neurotechnology, University Medical Center Göttingen, Georg August University, Göttingen, Germany
Corresponding author.
Address for reprint requests and other correspondence: D. Farina, Universitätsmedizin Göttingen, Georg-August-Universität, Dept. of Neurorehabilitation Engineering, Bernstein Focus Neurotechnology Göttingen, Bernstein Center for Computational Neuroscience, Von-Siebold-Str. 6, D-37075 Göttingen, Germany (e-mail: dario.farina@bccn.uni-goettingen.de).

Received 2015 Apr 22; Accepted 2015 May 22.

Abstract

It has been observed that muscle pain influences force variability and low-frequency (<3 Hz) oscillations in the neural drive to muscle. In this study, we aimed to investigate the effect of experimental muscle pain on the neural control of muscle force at higher frequency bands, associated with afferent feedback (alpha band, 5–13 Hz) and with descending cortical input (beta band, 15–30 Hz). Single-motor unit activity was recorded, in two separate experimental sessions, from the abductor digiti minimi (ADM) and tibialis anterior (TA) muscles with intramuscular wire electrodes, during isometric abductions of the fifth finger at 10% of maximal force [maximum voluntary contraction (MVC)] and ankle dorsiflexions at 25% MVC. The contractions were repeated under three conditions: no pain (baseline) and after intramuscular injection of isotonic (0.9%, control) and hypertonic (5.8%, painful) saline. The results showed an increase of the relative power of both the force signal and the neural drive at the tremor frequency band (alpha, 5–13 Hz) between the baseline and hypertonic (painful) conditions for both muscles ($P < 0.05$) but no effect on the beta band. Additionally, the strength of motor unit coherence was lower ($P < 0.05$) in the hypertonic condition in the alpha band for both muscles and in the beta band for the ADM. These results indicate that experimental muscle pain increases the amplitude of the tremor oscillations because of an increased variability of the neural control (common synaptic input) in the tremor band. Moreover, the concomitant decrease in coherence suggests an increase in independent input in the tremor band due to pain.

Keywords: motor unit, experimental muscle pain, tremor, motor unit coherence

ALPHA MOTOR NEURONS receive common synaptic inputs from spinal and supraspinal sources during the execution of sustained contractions (Farina et al. 2014b). For this reason, motor neuron spike trains show some level of correlation, which can be estimated with time (cross-correlation) (De Luca et al. 1982; Nordstrom et al. 1992) or frequency (coherence) domain (Farmer et al. 1993; Myers et al. 2004) methods. In addition to low-frequency components (common drive) (De Luca et al. 1982), the effective control signal to the muscle is also partly reflected in the alpha band (5–13 Hz), which is commonly associated with involuntary oscillations, termed physiological tremor (McAuley and Marsden 2000). Common input

in this frequency band is also reflected in the variability of force, since these neural oscillations are not fully filtered out by the contractile properties of muscles (Baldissera et al. 1998). Higher common frequencies (beta band) are believed to be related to the monosynaptic corticospinal projections (Halliday et al. 1999; Negro and Farina 2011a), but their direct influence on force output is probably negligible because of the severe muscle low-pass filtering (Negro and Farina 2011b; Farina and Negro 2015).

Nociception influences motor output, with effects ranging from decreased maximal force (Graven-Nielsen et al. 1997) to reduced force steadiness during submaximal tasks (Farina et al. 2012). The way in which tasks are executed is influenced by pain, but the influence depends on the demands of the task and on the constraints imposed to execute the task. For this reason, studies analyzing different tasks have observed a different change in task accuracy (e.g., force steadiness) in painful conditions (e.g., Bandholm et al. 2008; Farina et al. 2004, 2012; Smith et al. 2006). A large intersubject variability of the influence of muscle pain in force control is also often reported (Hodges and Moseley 2003; Sae-Lee et al. 2008).

Previously, we observed that the impaired ability to maintain a constant force during an unaccustomed task of the fifth digit with experimental muscle pain was mediated by an increase in the amplitude of oscillations of the common low-frequency components (<3 Hz) of motor unit spike trains (Farina et al. 2012). The increased variability in these components reflects greater variability in the common synaptic input received by the motor neurons at low frequency. The steadiness of this low-frequency component is controlled by the integration of supraspinal (descending drive) input and afferent synaptic input. Thus a high variability of the low-frequency component may suggest a suboptimal compensation of afferent input by the descending drive due to nociceptive stimulation. In this study, we focus on the influence of experimental muscle pain on higher frequency bands of the neural drive to muscle. The results of the study contribute to the understanding of the influence of pain on the execution of fine motor tasks as controlling contraction of a muscle at targeted force.

MATERIALS AND METHODS

Subjects. Data from 23 healthy subjects were analyzed. All subjects were right hand dominant, and none reported symptoms of neuromuscular disorders or musculoskeletal pain. Ethical approval for the study was granted by the Ethics Committee of Nordjylland, Denmark (ref. N-20090019). Informed written consent was obtained from all participants, and the procedures were conducted in accordance with the Declaration of Helsinki.

Signal recording. For the present study, we reanalyzed the intramuscular electromyography (iEMG) data reported in two previous studies (Farina et al. 2004, 2012) that investigated the discharge properties of motor units during experimental pain in the abductor digiti minimi (ADM) (11 subjects, *experiment 1*) and tibialis anterior (TA) (12 subjects, *experiment 2*) muscles. In both experiments, single-motor unit action potentials were recorded with sterilized Teflon-coated stainless steel intramuscular wire electrodes (diameter 0.1 mm; A-M Systems, Carlsborg, WA). The wires were cut to expose the cross section of the tip without insulation. After disinfection of the skin, the wires were inserted into the muscle belly via a 25-gauge hypodermic needle, which was removed immediately after the insertion, leaving the wire electrodes inside the muscle. The bipolar iEMG signals were amplified (Counterpoint EMG, Dantec Medical, Skovlunde, Denmark) with a gain of 500, band-pass filtered between 500 Hz and 5,000 Hz, and sampled at 10,000 samples/s for both experiments. A reference electrode was placed around the right wrist in *experiment 1* and the right ankle in *experiment 2*.

The fifth digit abduction force (ADM) and ankle dorsiflexion force (TA) were recorded and used for online visual feedback for the subjects in both experiments. Since highly accurate decomposition of a relatively high number of motor units is required for coherence analysis, the analysis of the final results was obtained only from the most accurate decomposed data that corresponded to 9 of 11 subjects (9 men; age 25.1 ± 2.5 yr) for the ADM muscle and 7 of 12 subjects (7 men; age 24.2 ± 2.1 yr) for the TA muscle. Decompositions with abnormal interspike intervals (ISIs) due to a high incidence of missed or wrongly matched discharges were excluded. This was judged by researchers through visual examination of the decomposition results. Decompositions with ISIs outside physiological limits were excluded (Moritz et al. 2005).

Experimental muscle pain.

In both experiments, experimental muscle pain was induced by injection (27-gauge cannula) of 0.5 ml of sterile hypertonic saline (5.8%). Isotonic saline (0.5 ml, 0.9%) was used as a control injection. The injections into the ADM were performed manually, and the bolus was delivered over 10 s. The location of the injection was ~10 mm distal and ~5 mm transverse to the intramuscular wires. Participants were asked to verbally rate their level of perceived pain intensity on an 11-point numerical rating scale (NRS) anchored with "no pain" (0) and "the worst possible pain imaginable" (10) every 30 s until pain was no longer reported. In the second experiment, a computer-controlled syringe pump (IVAC, model 770) was used to infuse the saline into the TA muscle over 40 s. The location of the needle was ~10 mm transverse to the intramuscular wires. The level of perceived pain intensity was rated by the subjects every 5 s until pain was no longer reported.

Experiment 1. Participants were seated on an adjustable chair with the right arm and the first four digits fixed on a force measuring device with Velcro straps. The fifth finger was fixed to a load cell to measure isometric abduction force. The participants performed three maximum voluntary contractions (MVCs) of right fifth finger abduction with 2-min rest intervals between trials. Verbal encouragement was provided to the subject to promote higher forces in each trial. The highest value of force recorded was selected as the reference MVC. After the MVC recordings, the participants performed one sustained abduction of the fifth finger at 10% of MVC for 60 s under three conditions: baseline, isotonic saline, and hypertonic saline. Visual feedback of finger abduction force was provided on an oscilloscope. The participants were asked to keep the force signal at the target level that was provided as visual feedback (resolution adjusted as ±10% of the target force) as accurately as possible. The order of the baseline and isotonic saline conditions was randomized across subjects, and they were followed finally by the hypertonic saline condition. A rest of 5 min was given between conditions.

Experiment 2. The participants were seated in a comfortable chair with their ankle at 90° of flexion, knee at 120° of extension, and hip at 90° of flexion and with their foot fixed in an isometric force brace. The ankle dorsiflexion force was measured with a torque transducer that was incorporated in the isometric force plate (Aalborg University, Aalborg, Denmark). In this experiment, the same procedure was applied in the same experimental session on both legs, apart from the type of infusion [hypertonic saline in the right leg (painful condition); isotonic saline in the left leg (control condition)].

Subjects performed three MVCs of ankle dorsiflexion with 2-min rest between contractions. Verbal encouragement was provided to the subject to promote higher forces in each trial, and the highest value of force was selected as the reference MVC. After 5 min of rest, subjects performed sustained isometric dorsiflexion for 4-min at 25% MVC. Visual feedback of ankle dorsiflexion force was provided on an oscilloscope. The participants were asked to keep the force signal at the target level that was provided as visual feedback (resolution adjusted as ±10% of the target force) as accurately as possible. The subject then had a 20-min rest, after which hypertonic (right leg) or isotonic (left leg) saline was infused. Two minutes after the beginning of the infusion, the subject was asked to perform a 4-min-long contraction at 25% MVC, identical to the previous one. Thus a total of four contractions, two for each leg, were performed by the subject with and without injection of saline. The order of assessment of the two legs was randomized. For the present study, a data segment of 60-s duration in the interval of maximum pain was decomposed and analyzed.

Signal and data analysis. iEMG signals were filtered with a 1,000-Hz high-pass filter and decomposed with the EMGLAB decomposition program (McGill et al. 2005). Furthermore, each motor unit spike train was manually edited with the visual interface of the program for inspecting unusually long or short ISIs. The motor units were discriminated from the segment of iEMG where the signal quality was high enough to provide a reliable decomposition and where the highest level of perceived pain intensity was approximately constant.

The discharge properties of motor units, coherence, power spectrum, and statistical analysis were performed with custom-designed software written in MATLAB (MathWorks, Natick, MA). After decomposition, the smoothed spike trains (Fig. 1) were examined for each trial to eliminate the motor unit spike trains that had abnormally low or high ISIs (Semmler 2002).

The force signal was preprocessed by applying a low-pass filter with 20-Hz cutoff frequency after removing the offset. To examine the strength of force oscillations in the three conditions (baseline, isotonic, and pain), the standard deviation and power spectral density (PSD) of the force signal were computed from intervals of 5 s and 0.5 s, respectively. Welch's method (Welch 1967) was used for PSD estimation of the force signal, windowed with Hamming function without overlap. Additionally, to investigate the distribution of power over frequency for the neural drive to muscle, the PSD of the cumulative spike trains (CST) was calculated by a method similar to that for the force signal.

To estimate the relative proportion of common input with respect to independent input to motor units in each condition (baseline, hypertonic, isotonic), coherence analysis was performed on the CST for each subject and condition individually. The magnitude of the coherence function increases quadratically with the number of motor unit spike trains considered in the CST, resulting in better estimates (Farina et al. 2014a; Negro and Farina 2011a). In the present study, the number of decomposed motor units was only four in some cases. Therefore, the CST was calculated from the possible unique combinations of motor unit pairs (Fig. 2). In this way, all conditions were analyzed with the same number of motor units, so that the coherence values could be compared between conditions (Negro and Farina 2012).

To compute the coherence function, the Welch's averaged, modified periodogram method was used:

$$k(\omega) = \frac{|X_{ij}(\omega)|^2}{\sqrt{X_{ii}(\omega)\, X_{jj}(\omega)}} \quad (1)$$

where $X_{ij}(\omega)$ is the cross-spectrum (the Fourier transform of the cross-correlation function) of the two CSTs and $X_{ii}(\omega)$ and $X_{jj}(\omega)$ the respective autospectra. The discriminated spike trains were divided into nonoverlapping 0.5-s windows (Hamming) with a length for the fast Fourier transform (FFT) of 10 times sampling rate (10 × Fs) (zero padding). To define the significance threshold for coherence peaks, the confidence level was calculated as (Rosenberg et al. 1989):

$$\mathrm{CL} = 1 - (1 - \alpha)^{\frac{1}{N-1}} \quad (2)$$

where N and α represent the number of segments used in the coherence calculation (data length/number of windows) and the confidence level (95%), respectively.

The Fisher's z-transform was applied to the coherence values and confidence level in order to compare the normalized coherence values between the three conditions (Laine et al. 2014; Rosenberg et al. 1989). The integration of coherence values over the confidence level, which is an indication of synchronization of motor units, was calculated for the 2–50 Hz frequency band.

To compare the strength of coherence, the PSD of force and of the CST, relative to the total power (averaged on 2-Hz bin size), repeated-measures ANOVA was used with two factors (frequency and conditions) for both muscles. The Tukey's honestly significant difference (HSD) post hoc analysis was used to define differences between conditions in specific frequency bands. The difference between the subjective pain scores (NRS), number of motor units, mean discharge rate, coefficient of variation (CoV) of ISI, and CoV of force in the three conditions was investigated by a one-way ANOVA for both muscles. Significant differences revealed by ANOVA were followed by post hoc Fisher's least significant difference (LSD) pairwise comparisons. Statistical significance was set at $P < 0.05$.

RESULTS

Experimental pain scores. The injection of hypertonic saline elicited a significant painful sensation for both muscles. The peak pain intensity, as measured by the NRS score, was greater after the injection of hypertonic saline (ADM: 4.4 ± 2.1; TA: 3.5 ± 1.2) compared with isotonic saline (ADM: 1.0 ± 0.4; TA: 0.3 ± 0.1) in both muscles ($P < 0.05$) (Table 1). The NRS scores were 4.7 ± 1.8 and 4.2 ± 1.9 for the ADM and

3.8 ± 1.2 and 3.4 ± 1.0 for the TA in the hypertonic saline condition at the beginning and the end of the 60-s interval, respectively. The painful sensation did not change over time during the 60-s interval of analysis ($P > 0.05$) for both muscles.

Motor unit properties. The discharge properties of motor units were compared under the three conditions for both ADM and TA muscles. A total of 165 and 134 individual motor units were identified from the ADM and TA muscles, respectively. Motor unit discharge rates were not significantly different between conditions for both ADM ($P = 0.185$) and TA ($P = 0.061$) muscles, although there was a tendency for lower rates in the hypertonic saline condition (Table 1). No significant differences in the number of analyzed motor units were found between conditions for the ADM ($P = 0.367$) and TA ($P = 0.257$) muscles. The CoVs of ISI for the ADM and TA muscles were not significantly different across conditions (Table 1).

Force. Variability of the force increased after the injection of hypertonic saline. The standard deviation of force was significantly greater for the hypertonic saline condition of both muscles (ADM: $P < 0.01$; TA: $P < 0.01$). Repeated-measures ANOVA showed a significant effect for condition ($P < 0.01$) and an interaction between frequency and condition ($P < 0.01$). The post hoc test revealed that the power of the force signal was greatest in the 4–8 Hz (tremor oscillation) and 2–4 Hz (common drive oscillation) frequency bands for both muscles ($P < 0.05$) during the hypertonic saline condition with respect to the other two conditions. For the TA muscle, the power of force was higher in the isotonic saline condition than baseline despite higher power during the hypertonic saline condition (Fig. 3). In line with these results, the relative variability of the force signal (CoV of force) depended on the condition for both muscles (ADM: $P < 0.05$; TA: $P < 0.05$). Post hoc analysis revealed that the CoV of force was greater in the hypertonic saline condition compared with both baseline (ADM: $P < 0.05$; TA: $P < 0.05$) and isotonic saline (ADM: $P < 0.01$; TA: $P < 0.01$) conditions (Table 1).

Composite spike train. The CST was examined in the frequency domain, as an estimate of the neural drive to the muscle. Repeated-measures ANOVA revealed a significant interaction between frequency and condition ($P < 0.01$). The post hoc test revealed that the relative power (PSD of the smoothed CST divided by the integral of the PSD function) of the neural drive to the muscle in the hypertonic (painful) saline condition was significantly greater than in the baseline condition in the lower frequency band (2–4 Hz) for both muscles ($P < 0.05$), as previously shown (Farina et al. 2012). Moreover, the hypertonic saline condition was associated with greater power of the CST also in the frequency interval from 8 to 12 Hz for the ADM muscle ($P < 0.01$) and from 6 to 12 Hz for the TA muscle ($P < 0.01$) (alpha band) (Fig. 4). No effect of experimental pain was observed for higher frequencies ($P > 0.10$).

Motor unit coherence. The influence of experimental muscle pain on the common input to motor units was investigated by calculating the coherence between CST. An average of 31 CST pairs per subject (intervals: 3–45 for baseline, 3–100 for hypertonic, and 15–100 for isotonic conditions) were calculated for the TA and 33 CST pairs (intervals: 3–45 for baseline, 3–100 for hypertonic, and 6–100 for isotonic conditions) for the ADM.

Representative examples of coherence estimates are shown in Fig. 5, *A* and *B*. In these examples, the coherence functions present a low-frequency component in the 2–4 Hz band, a narrow peak in the 6–10 Hz band, and a broad and lower peak in the 15–25 Hz band. Repeated-measures ANOVA revealed that, for both muscles, the strength of coherence between motor units was affected by condition ($P < 0.05$) and that there was an interaction between frequency and condition ($P < 0.05$). The strength of coherence between motor units in the hypertonic saline condition was significantly lower than in the other two conditions in the 6–8 Hz (ADM: $P < 0.05$; TA: $P < 0.05$) and 8–10 Hz (ADM: $P < 0.01$; TA: $P < 0.01$; Fig. 5, *C* and *D*) bands. Moreover, for the ADM muscle only, a significantly lower coherence strength in the hypertonic condition was observed with respect to the baseline and isotonic saline conditions at the frequencies 14–18 Hz (beta band) ($P < 0.05$; Fig. 5*C*). The coherence strength was significantly lower in the hypertonic saline condition compared with the baseline condition for the frequencies 18–22 Hz for ADM and 14–22 Hz for TA muscles; however, the hypertonic saline condition was not different with respect to the isotonic saline condition at these frequencies. No significant difference was found in the low frequency band (2–4 Hz) between conditions for both muscles ($P > 0.05$).

To confirm that the present results were not influenced by the average discharge rates of the analyzed motor units, the correlation between discharge rate of motor units and their strength of coherence at the analyzed frequency bands in the three conditions was calculated, and no significant correlation between the two variables was found for the ADM ($P = 0.30$) or TA ($P = 0.06$) muscles.

The integral of the coherence function in the full bandwidth (2–50 Hz), which is associated with the strength of short-term synchronization (Semmler et al. 2004), was lower in the hypertonic saline condition compared with both baseline and isotonic conditions for both muscles (ADM: $P < 0.05$; TA: $P < 0.05$) (Table 1).

DISCUSSION

Experimental muscle pain increased the physiological tremor component in the neural drive to muscle but did not influence the components in the beta band.

Consistent with previous observations in experimental (Bandholm et al. 2008; Farina et al. 2012) and clinical (Falla et al. 2010; Muceli et al. 2011) pain conditions, we observed a higher variability in the force oscillations (increased standard deviation of the force signal) in the hypertonic (painful) saline condition for both muscles. The high variability in the force signal indicates an impairment of the central nervous system to accurately control force when a nociceptive stimulus is present (Farina et al. 2012). Previous work has shown that the low-frequency oscillations (<3 Hz) of the motor unit spike trains increase during experimental muscle pain, impairing force steadiness (Farina et al. 2012). This frequency band represents the largest common input variation and is highly correlated with force fluctuations (Negro et al. 2009). In the present study, we showed that the delta band (2–4 Hz) of the neural drive to muscle had the highest power during pain, which confirms these earlier observations, and we extended the analysis to the full frequency bandwidth of the neural drive. The most consistent finding was an increased power (i.e., variability) of the neural drive to muscle in the alpha (tremor) frequency band (5–13 Hz) and a decreased motor unit coherence in the same band for both muscles. These changes in the neural drive to muscle corresponded to an increase in the force oscillations in the tremor frequency band.

Force oscillations in the alpha band (physiological tremor) increased during the hypertonic saline condition in both muscles. This observation is consistent with earlier work (Jaberzadeh et al. 2003) that documented a similar increase in physiological tremor (force signal) with experimental muscle pain induced in the extensor digitorum longus muscle. Previous studies demonstrated that tremor oscillations in force (6–10 Hz) are highly correlated with the activity of muscle spindle afferents (Halliday and Redfearn 1958; Laine et al. 2013, 2014; Lippold 1970). For this reason, an increase in the amplitude of the oscillations of the control signal (combination of cortical and afferent projections) would likely also increase the oscillations of the neural drive that are associated with the tremor frequency of the force spectrum. Indeed, the results of the present study showed that the relative power of the CST signal in the tremor band was greatest during the hypertonic saline condition.

Motor unit spike trains recorded during sustained isometric contractions show common oscillations in the delta, alpha, and beta frequency bands (Grosse et al. 2002). In these frequency bands, the shared synaptic projections over the motor neuron pool generate a significant level of coherence between multiple spike trains (Lowery et al. 2007; Negro and Farina 2011a). The coherent oscillations in the delta and alpha bands are transmitted to the force signal, whereas those at higher frequencies are filtered by the contractile properties of the muscle (Baldissera et al. 1998; Halliday et al. 1999).

The magnitude of the coherence between motor unit spike trains in the alpha band (6–10 Hz) significantly decreased in the presence of experimental muscle pain. This result was consistent in both the ADM and TA muscles and suggests that nociceptive afferent input may influence the relative strength of the common input with respect to the independent synaptic input to motor neurons in the tremor band. Oscillations in the alpha band are known to be influenced by the modulation of muscle spindle activity, e.g., under ischemic conditions (Erimaki and Christakos 2008) and muscle stretching (Negro et al. 2012; Semmler 2002). Specifically, results from previous studies have shown that the coherence between motor units increases with increasing muscle spindle activity. It is relevant to note that increased force signal power in the alpha band is not in contradiction with a decrease in motor unit coherence in the same bandwidth, since coherence expresses the relative strength of the correlation in the synaptic input but not its power (Farina

and Negro 2015; Halliday et al. 1995; Mima et al. 1999). Additionally, it has been shown that, while experimental muscle pain increases the stretch reflex amplitude, the H reflex is not influenced (Matre et al. 1998), which suggests that experimental muscle pain directly provokes muscle spindle activity rather than modulating muscle spindle afferent input presynaptically. Together with the results from the PSD analysis, one possible interpretation can be that pain increased both the power of the common oscillatory inputs to motor neurons at the tremor band (increased PSD of neural drive) that caused increased force oscillations at the same frequencies as well as the relative power of independent input with respect to common input (decreased coherence). The increased activity of monosynaptic muscle spindles during pain would increase the common synaptic input to motor neurons in the tremor band as discussed above. Despite this, the increase in strength of the independent input (synaptic noise) relative to the common synaptic input to motor neurons in the alpha band may be due to the fact that nociceptive afferents have polysynaptic innervation on motor units (Andersen et al. 2000). Therefore this polysynaptic input may have increased the strength of independent input due to the nonuniform synaptic distribution (Jankowska and Roberts 1972; Powers and Binder 1985) that may have divergent projections on the motor neuron pool.

In addition to the alpha band, the coherence values in the 14–22 Hz band (beta band) were lower in the hypertonic saline condition with respect to the baseline condition but only for the ADM muscle. Coherence peaks in the beta band are thought to be mostly associated with the firing oscillations generated by the motor and somatosensory cortex (Conway et al. 1995; Farmer et al. 1993; Halliday et al. 1999). Thus a decrease in coherence in the beta band can be interpreted as a reduction of the common input from the motor and somatosensory cortex to the motor neuron pool due to pain. The observation that hand muscles have broader corticospinal projections to their motor neuron pools compared with leg muscles (Brouwer and Ashby 1990) may explain the lack of this effect in the TA muscle.

The average motor unit discharge rate influences the estimation of coherence magnitude (Christou et al. 2007). In this study, motor unit discharge rates decreased with pain (Farina et al. 2004, 2012), although not significantly. Moreover, the mean motor unit discharge rate was not correlated with the magnitude of the estimated coherence, in all three conditions and for both muscles, which excludes an influence of discharge rate on the conclusions drawn.

In conclusion, we observed a higher variability of force and greater oscillations of the neural drive to the muscles in the tremor band during the hypertonic saline (painful) condition with respect to isotonic and baseline conditions. At the same time, the coherence in the same frequency band decreased, suggesting a relatively greater increase in independent inputs (synaptic noise) to motor neurons with respect to the increase in common input oscillations. Therefore, one interpretation of the present results can be that muscle pain increases the power of both common inputs to motor neurons, which are translated into greater force oscillations, and of independent input.

GRANTS

This study is supported by European Research Council Advanced Grant DEMOVE No. 267888.

DISCLOSURES

No conflicts of interest, financial or otherwise, are declared by the author(s).

AUTHOR CONTRIBUTIONS

Author contributions: U.Ş.Y., F.N., D. Falla, and D. Farina conception and design of research; U.Ş.Y. analyzed data; U.Ş.Y., F.N., D. Falla, and D. Farina interpreted results of experiments; U.Ş.Y. prepared figures; U.Ş.Y., F.N., D. Falla, and D. Farina drafted manuscript; U.Ş.Y., F.N., D. Falla, and D. Farina edited and revised manuscript; U.Ş.Y., F.N., D. Falla, and D. Farina approved final version of manuscript; F.N. and D. Farina performed experiments.

REFERENCES

Andersen O, Graven-Nielsen T, Dagfinn M, Arendt-Nielsen L, Schomburg E. Interaction between cutaneous and muscle afferent activity in polysynaptic reflex pathways: a human experimental study. Pain 84: 29–36, 2000. [PubMed: 10601670]

Baldissera F, Cavallari P, Cerri G. Motoneuronal pre-compensation for the low-pass filter characteristics of muscle. A quantitative appraisal in cat muscle units. J Physiol 511: 611–627, 1998. [PMCID: PMC2231136] [PubMed: 9706036]

Bandholm T, Rasmussen L, Aagaard P, Diederichsen L, Jensen BR. Effects of experimental muscle pain on shoulder-abduction force steadiness and muscle activity in healthy subjects. Eur J Appl Physiol 102: 643–650, 2008. [PubMed: 18066578]

Brouwer B, Ashby P. Corticospinal projections to upper and lower limb spinal motoneurons in man. Electroencephalogr Clin Neurophysiol 76: 509–519, 1990. [PubMed: 1701119]

Christou EA, Rudroff T, Enoka JA, Meyer F, Enoka RM. Discharge rate during low-force isometric contractions influences motor unit coherence below 15 Hz but not motor unit synchronization. Exp Brain Res 178: 285–295, 2007. [PubMed: 17091298]

Conway BA, Halliday DM, Farmer SF, Shahani U, Maas P, Weir AI, Rosenberg JR. Synchronization between motor cortex and spinal motoneuronal pool during the performance of a maintained motor task in man. J Physiol 489: 917–24, 1995. [PMCID: PMC1156860] [PubMed: 8788955]

Erimaki S, Christakos CN. Coherent motor unit rhythms in the 6–10 Hz range during time-varying voluntary muscle contractions: neural mechanism and relation to rhythmical motor control. J Neurophysiol 99: 473–483, 2008. [PubMed: 18057114]

Falla D, Lindstrøm R, Rechter L, Farina D. Effect of pain on the modulation in discharge rate of sternocleidomastoid motor units with force direction. Clin Neurophysiol 121: 744–753, 2010. [PubMed: 20097603]

Farina D, Arendt-Nielsen L, Merletti R, Graven-Nielsen T. Effect of experimental muscle pain on motor unit firing rate and conduction velocity. J Neurophysiol 91: 1250–1259, 2004. [PubMed: 14614105]

Farina D, Merletti R, Enoka RM. The extraction of neural strategies from the surface EMG: an update. J Appl Physiol 117: 1215–1230, 2014a. [PMCID: PMC4254845] [PubMed: 25277737]

Farina D, Negro F. Common synaptic input to motor neurons, motor unit synchronization, and force control. Exerc Sport Sci Rev 43: 23–33, 2015. [PubMed: 25390298]

Farina D, Negro F, Dideriksen JL. The effective neural drive to muscles is the common synaptic input to motor neurons. J Physiol 592: 3427–3441, 2014b. [PMCID: PMC4229341] [PubMed: 24860172]

Farina D, Negro F, Gizzi L, Falla D. Low-frequency oscillations of the neural drive to the muscle are increased with experimental muscle pain. J Neurophysiol 107: 958–965, 2012. [PMCID: PMC3289482] [PubMed: 22049336]

Farmer SF, Bremner FD, Halliday DM, Rosenberg JR, Stephens JA. The frequency content of common synaptic inputs to motoneurones studied during voluntary isometric contraction in man. J Physiol 470: 127–155, 1993. [PMCID: PMC1143910] [PubMed: 8308721]

Graven-Nielsen T, Svensson P, Arendt-Nielsen L. Effects of experimental muscle pain on muscle activity and co-ordination during static and dynamic motor function. Electroencephalogr Clin Neurophysiol 105: 156–164, 1997. [PubMed: 9152211]

Grosse P, Cassidy MJ, Brown P. EEG-EMG, MEG-EMG and EMG-EMG frequency analysis: physiological principles and clinical applications. Clin Neurophysiol 113: 1523–1531, 2002. [PubMed: 12350427]

Halliday AM, Redfearn JW. Finger tremor in tabetic patients and its bearing on the mechanism producing the rhythm of physiological tremor. J Neurol Neurosurg Psychiatry 21: 101–108, 1958. [PMCID: PMC497303] [PubMed: 13539651]

Halliday DM, Conway BA, Farmer SF, Rosenberg JR. Load-independent contributions from motor-unit synchronization to human physiological tremor. J Neurophysiol 82: 664–675, 1999. [PubMed: 10444664]

Halliday DM, Rosenberg JR, Amjad AM, Breeze P, Conway IB, Farnier SF. A framework for the analysis of mixed time series point process data—theory and application to the study of physiological tremor, single motor unit discharges and electromyograms. Prog Biophys Mol Biol 64: 237–278, 1995. [PubMed: 8987386]

Hodges PW, Moseley GL. Pain and motor control of the lumbopelvic region: effect and possible mechanisms. J Electromyogr Kinesiol 13: 361–370, 2003. [PubMed: 12832166]

Jaberzadeh S, Svensson P, Nordstrom MA, Miles TS. Differential modulation of tremor and pulsatile control of human jaw and finger by experimental muscle pain. Exp Brain Res 150: 520–524, 2003. [PubMed: 12739086]

Jankowska E, Roberts W. Synaptic actions of single interneurones mediating reciprocal Ia inhibition of motoneurones. J Physiol 222: 623–642, 1972. [PMCID: PMC1331404] [PubMed: 5033026]

Laine CM, Negro F, Farina D. Neural correlates of task-related changes in physiological tremor. J Neurophysiol 110: 170–176, 2013. [PubMed: 23596333]

Laine CM, Yavuz SU, Farina D. Task-related changes in sensorimotor integration influence the common synaptic input to motor neurones. Acta Physiol (Oxf) 211: 229–239, 2014. [PubMed: 24620727]

Lippold OC. Oscillation in the stretch reflex arc and the origin of the rhythmical, 8–12 c/s component of physiological tremor. J Physiol 206: 359–382, 1970. [PMCID: PMC1348651] [PubMed: 5532249]

Lowery MM, Myers LJ, Erim Z. Coherence between motor unit discharges in response to shared neural inputs. J Neurosci Methods 163: 384–391, 2007. [PubMed: 17482677]

De Luca CJ, LeFever RS, McCue MP, Xenakis AP. Control scheme governing concurrently active human motor units during voluntary contractions. J Physiol 329: 129–142, 1982. [PMCID: PMC1224771] [PubMed: 7143247]

Matre DA, Sinkjaer T, Svensson P, Arendt-Nielsen L. Experimental muscle pain increases the human stretch reflex. Pain 75: 331–339, 1998. [PubMed: 9583769]

McAuley JH, Marsden CD. Physiological and pathological tremors and rhythmic central motor control. Brain 123: 1545–1567, 2000. [PubMed: 10908186]

McGill KC, Lateva ZC, Marateb HR. EMGLAB: an interactive EMG decomposition program. J Neurosci Methods 149: 121–133, 2005. [PubMed: 16026846]

Mima T, Simpkins N, Oluwatimilehin T, Hallett M. Force level modulates human cortical oscillatory activities. Neurosci Lett 275: 77–80, 1999. [PubMed: 10568503]

Moritz CT, Benjamin KB, Michael AP, Roger ME. Discharge rate variability influences the variation in force fluctuations across the working range of a hand muscle. J Neurophysiol 93: 2449–2459, 2005. [PubMed: 15615827]

Muceli S, Farina D, Kirkesola G, Katch F, Falla D. Reduced force steadiness in women with neck pain and the effect of short term vibration. J Electromyogr Kinesiol 21: 283–290, 2011. [PubMed: 21195628]

Myers LJ, Erim Z, Lowery MM. Time and frequency domain methods for quantifying common modulation of motor unit firing patterns. J Neuroeng Rehabil 1: 2, 2004. [PMCID: PMC544949] [PubMed: 15679910]

Negro F, Farina D. Linear transmission of cortical oscillations to the neural drive to muscles is mediated by common projections to populations of motoneurons in humans. J Physiol 589: 629–637, 2011a. [PMCID: PMC3055547] [PubMed: 21135042]

Negro F, Farina D. Transmission of cortical oscillations to motoneuron output for force control. Physiol News 84: 35–36, 2011b.

Negro F, Farina D. Factors influencing the estimates of correlation between motor unit activities in humans. PLoS One 7: e44894, 2012. [PMCID: PMC3458041] [PubMed: 23049762]

Negro F, Holobar A, Dario F. Fluctuations in isometric muscle force can be described by one linear projection of low-frequency components of motor unit discharge rates. J Physiol 587: 5925–5935, 2009. [PMCID: PMC2808549] [PubMed: 19840996]

Negro F, Yavuz U, Farina D. Coherence between motor unit spike trains in human tibialis anterior muscle is influenced by ankle joint angle (Abstract). 2012 Neuroscience Meeting Planner. New Orleans, LA: Society of Neuroscience, program no. 887.11, 2012.

Nordstrom MA, Fuglevand AJ, Enoka RM. Estimating the strength of common input to human motoneurons from the cross-correlogram. J Physiol 453: 547–574, 1992. [PMCID: PMC1175573] [PubMed: 1464844]

Powers RK, Binder MD. Distribution of oligosynaptic group I input to the cat medial gastrocnemius motoneuron pool. J Neurophysiol 53: 497–517, 1985. [PubMed: 2984351]

Rosenberg JR, Amjad AM, Breeze P, Brillinger DR, Halliday DM. The Fourier approach to the identification of functional coupling between neuronal spike trains. Prog Biophys Mol Biol 53: 1–31, 1989. [PubMed: 2682781]

Sae-Lee D, Whittle T, Forte AR, Peck CC, Byth K, Sessle BJ, Murray GM. Effects of experimental pain on jaw muscle activity during goal-directed jaw movements in humans. Exp Brain Res 189: 451–462, 2008. [PubMed: 18551286]

Semmler JG. Motor unit synchronization and neuromuscular performance. Exerc Sport Sci Rev 30: 8–14, 2002. [PubMed: 11800501]

Semmler JG, Sale MV, Meyer FG, Nordstrom MA. Motor-unit coherence and its relation with synchrony are influenced by training. J Neurophysiol 92: 3320–3331, 2004. [PubMed: 15269232]

Smith R, Pearce SL, Miles TS. Experimental muscle pain does not affect fine motor control of the human hand. Exp Brain Res 174: 397–402, 2006. [PubMed: 16642315]

Welch PD. The use of fast Fourier transform for the estimation of power spectra: a method based on time averaging over short, modified periodograms. IEEE Trans Audio Electroacoust 15: 70–73, 1967.

Figures and Tables

Fig. 1.

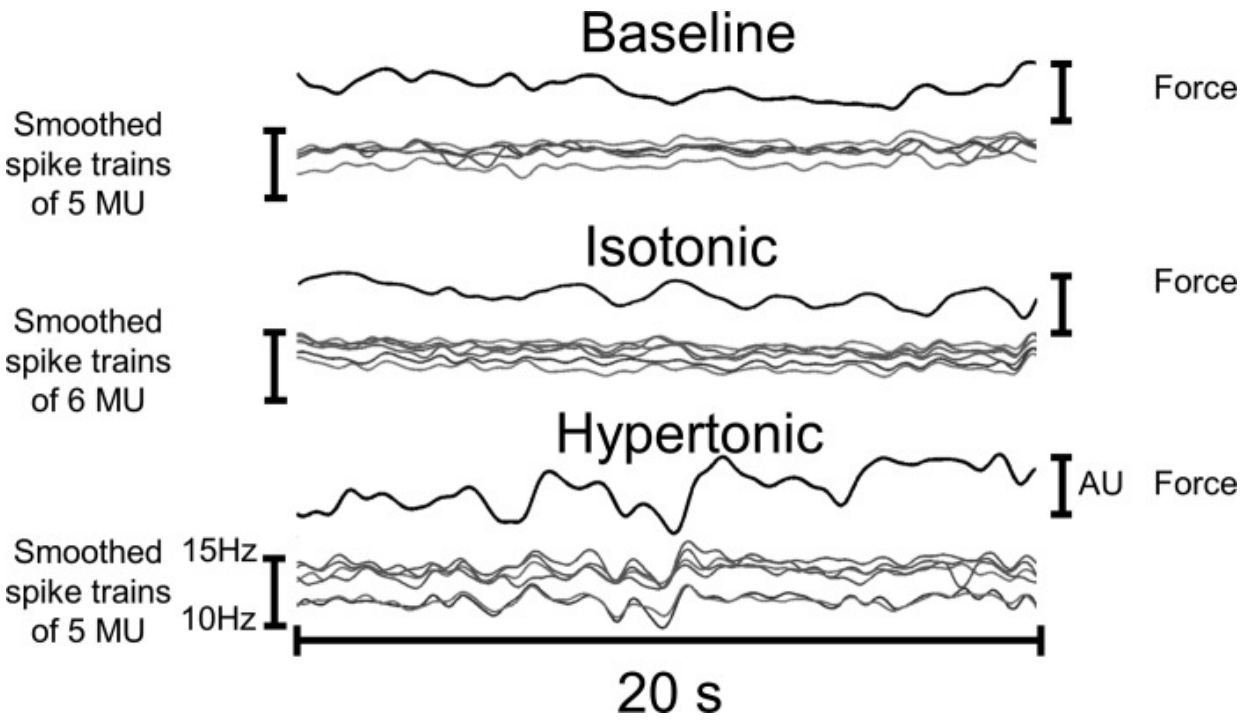

Smoothed spike trains from the abductor digiti minimi (ADM) muscle and force recorded from 1 representative subject during the baseline condition and after the injection of hypertonic and isotonic saline. *Top* trace in each condition denotes the force signal. Each trace in gray tone below the force trace denotes different motor units (MU). AU, arbitrary unit.

Fig. 2.

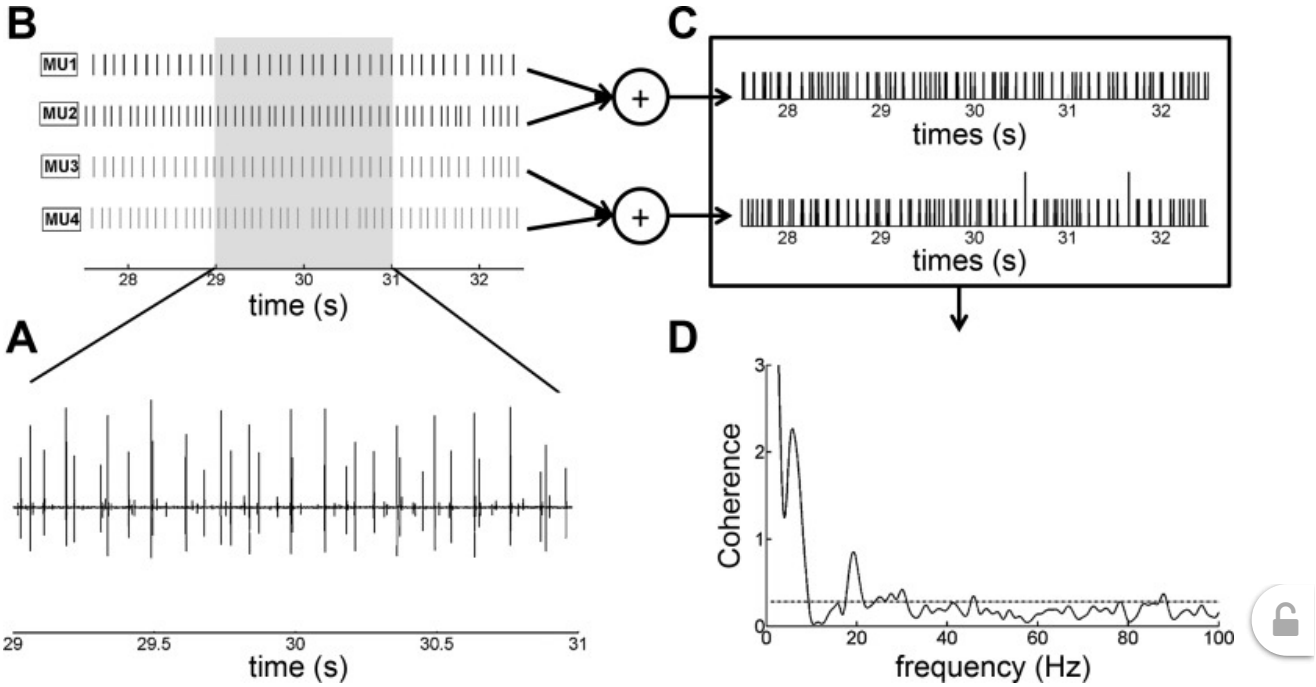

Estimation of coherence. *A*: the raw intramuscular signal was decomposed into single motor units (2-s interval of intramuscular signal). *B*: discharge times of the discriminated single motor units. *C*: composite spike trains (CST) were calculated from all possible unique combinations of 2 motor units (for the data segment of 60-s duration). *D*: the normalized coherence was estimated from the CST (dashed horizontal line indicates 95% confidence level).

Table 1.

Motor unit discharge rate, coefficient of variation of interspike interval and force, and integral value of coherence function for ADM and TA during baseline and after injection of hypertonic and isotonic saline

	ADM			TA		
	Baseline	**Hypertonic**	**Isotonic**	**Baseline**	**Hypertonic**	**Isotonic**
Pain (NRS)		4.4 ± 2.1*	1.0 ± 0.4		3.5 ± 1.2*	0.3 ± 0.1
No. of MUs	53	60	52	42	51	41
DR, spike/s	8.5 ± 1.5	7.9 ± 1.9	8.2 ± 2.2	8.3 ± 0.7	7.4 ± 1.4	8.0 ± 1.1
CoV of ISI, %	16 ± 4	16 ± 5	16 ± 5	11 ± 3	12 ± 5	11 ± 2
CoV of force, %	3.5 ± 1.6	3.8 ± 1.5*	3.5 ± 1.6	1.5 ± 0.6	2.0 ± 1.0*	1.6 ± 0.7
CohInt, Hz	304 ± 58	284 ± 61*	298 ± 58	290 ± 78	265 ± 64*	288 ± 68

Data are average ± SD values for motor unit (MU) discharge rate (DR), coefficient of variation (CoV) of the interspike interval (ISI) and force, and integral value of the coherence function between 2 Hz and 50 Hz (CohInt) for the abductor digiti minimi (ADM) and tibialis anterior (TA) muscles recorded during a baseline condition and after injection of hypertonic and isotonic saline. NRS, numerical rating scale.

*Significantly different in the hypertonic saline condition with respect to the baseline and isotonic saline conditions for the same muscle ($P < 0.05$).

Fig. 3.

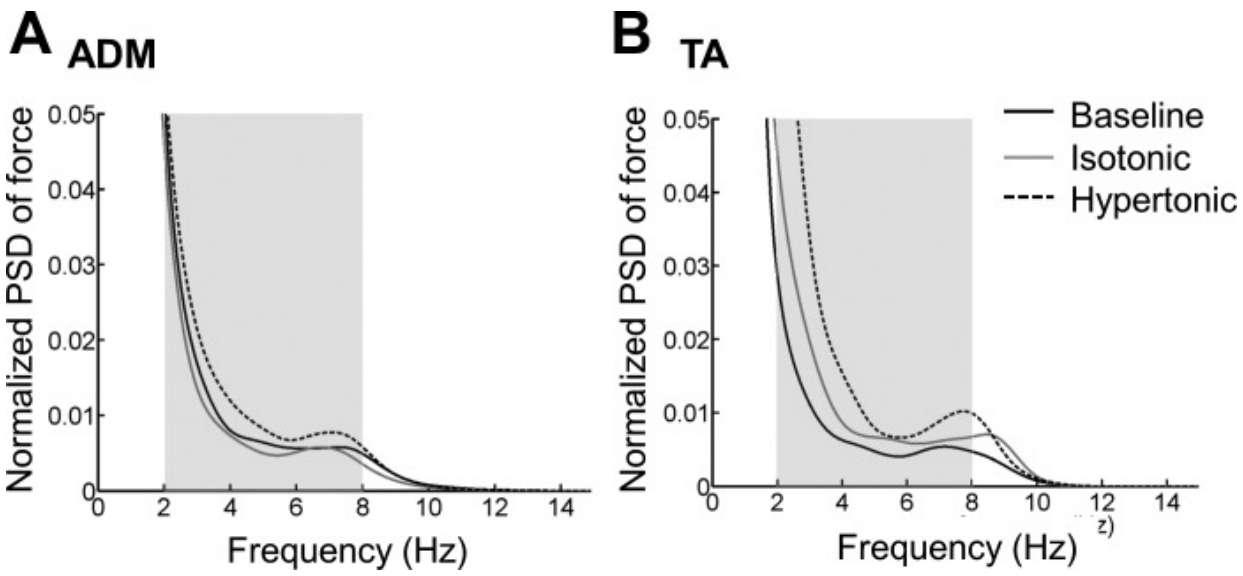

Averaged power spectrum density (PSD) estimates for the force signal of the ADM (*A*) and TA (*B*) muscles. Shaded area shows the frequency interval where significantly higher power was observed for the hypertonic saline condition compared with the other conditions ($P < 0.05$).

Fig. 4.

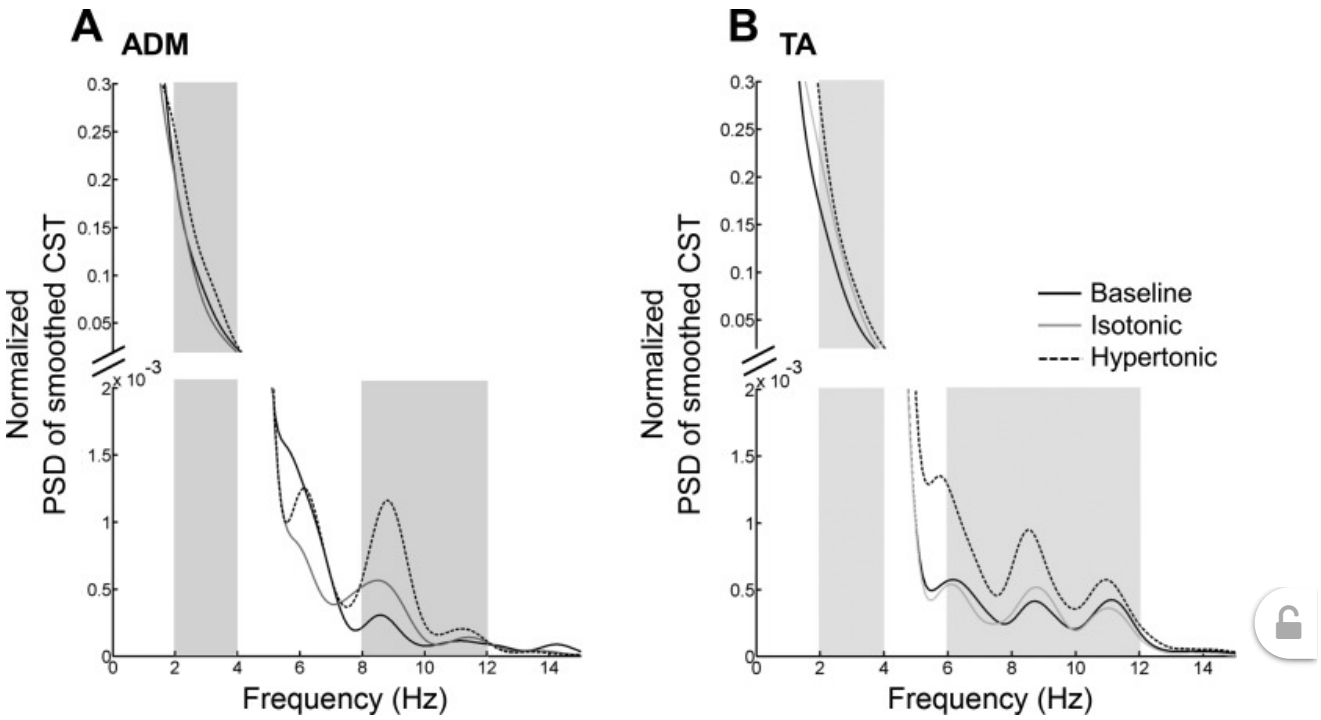

Averaged (over subjects) PSD estimations of smoothed CST in the time interval analyzed for the ADM (*A*) and TA (*B*) muscles. Shaded area shows the frequency interval where significantly higher power was observed for the hypertonic saline condition compared with the baseline condition. The PSD is shown only for the delta and alpha bands for clarity. No differences were detected among conditions for higher frequencies.

Fig. 5.

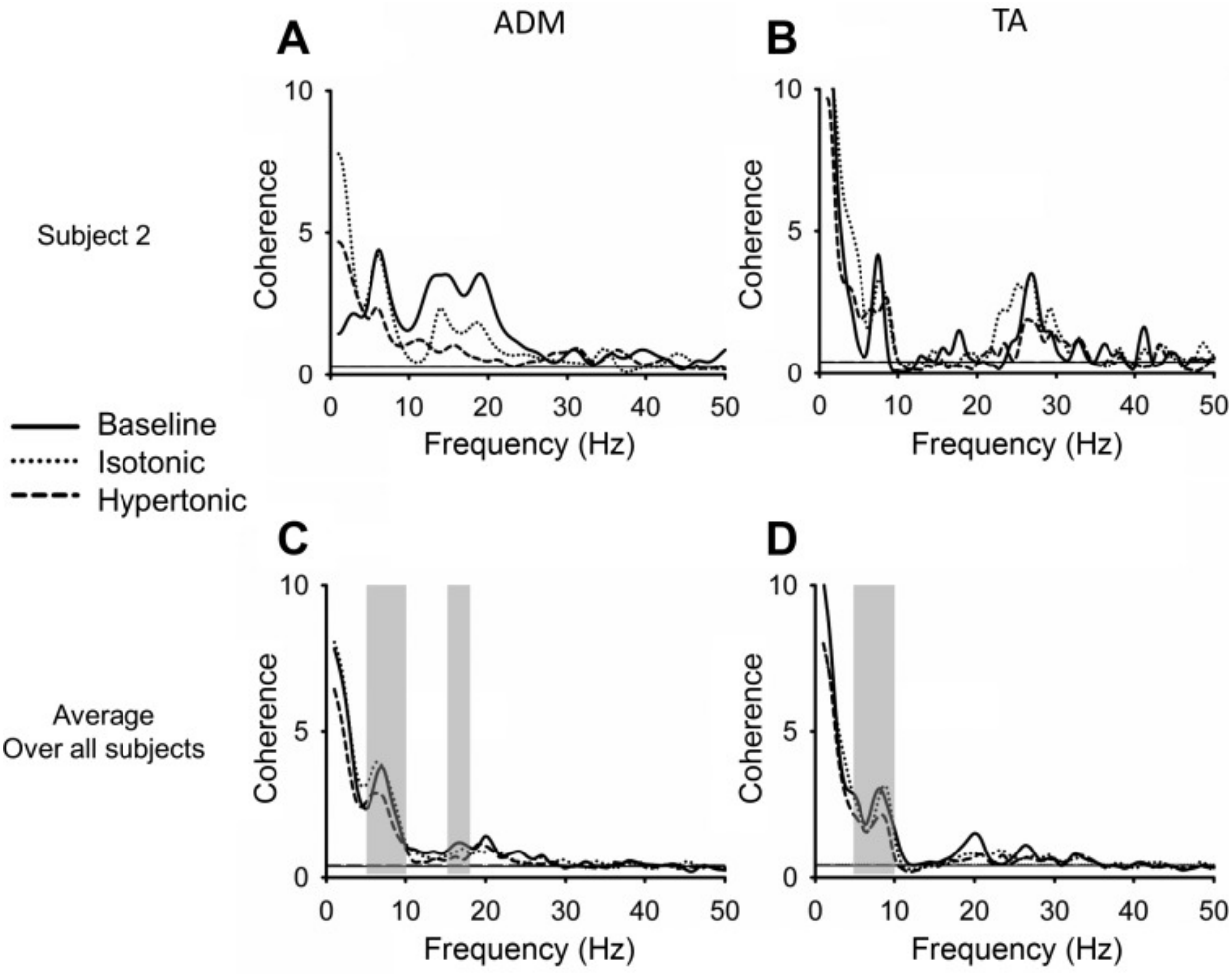

Coherence estimates for a representative subject and for the pooled data. *A*: coherence for the ADM muscle of *subject 2*. *B*: coherence for the TA muscle of *subject 2*. *C*: pooled coherence for the ADM muscle. *D*: pooled coherence for the TA muscle. Shaded areas show frequency bands where coherence was significantly lower in the hypertonic condition compared with the other conditions ($P < 0.05$). Horizontal lines (solid, dotted, and dashed) show the 95% confidence interval for all conditions. Coherence values are *z*-transformed.